APPLICATION OF NEURAL NETWORKS TO MODEL AND PREDICT ROTORCRAFT HUB LOADS

Sesi Kottapalli, Anita Abrego, and Stephen Jacklin
Rotorcraft Aeromechanics Branch
NASA Ames Research Center
Moffett Field, California

Abstract

Neural networks are applied to model and predict experimentally measured vibratory hub loads. Data from a wind tunnel test of a four-bladed hingeless rotor in forward flight (with individual blade control) were used to provide 2P and 3P control amplitude, control phase, and vibratory hub loads. A metric consisting of an equally weighted combination of five 4P vibratory hub loads was used to characterize the hub loads. Using the control phase and/or amplitude as inputs and the vibratory hub loads metric as output, the radial-basis function (RBF) and back-propagation types of networks were trained. The RBF network is robust for interpolative purposes, including significant nonlinearities. The RBF network also works well when there are multiple inputs and predictions of nonlinear non-baseline metrics (and accompanying baseline metrics). The back-propagation neural network is robust for interpolation, and with some guidance, produces acceptable extrapolations. The smallest number of RBF network training data pairs, i.e., that which results in the most efficient network, is found to depend on an input phase interval limit related to the physical rotor azimuth control angle. This control-angle-interval-limit of 30 deg rotor azimuth is believed to be linked to the basic physical phenomenon of vibratory hub loads for the blade vortex interaction (BVI) test condition studied. Finally, results show that RBF neural networks are superior to linear transfer matrix plant models for the experimental vibratory hub loads data presented in this paper.

Presented at the 2nd International Aeromechanics Specialists Conference, Bridgeport, Connecticut, October 11-13, 1995.

Notation

A	Rotor disk area, πR^2
A_m	Amplitude of mP IBC input, deg
b_k	Specified bias for kth processing element, same as w_{k0}
c	Representative chord of the blade
C_T	Rotor thrust coefficient, thrust nondimensionalized by $\rho A(\Omega R)^2$
i	Blade number; i=1 implies ψ=0 for blade at helicopter tail
IBC	Individual Blade Control
m	Harmonic number for IBC input
N_b	Number of blades
R	Rotor blade radius
V	Wind tunnel airspeed, knots
w_{kn}	weight for nth input in the kth processing element
x_n	Input to processing element, n=0,1,2 ...p
y_k	Output of kth processing element
α_s	Rotor shaft angle, positive nose up, deg
θ_{im}	IBC contribution to blade pitch, mth harmonic pitch for ith blade
μ	advance ratio, $V/(\Omega R)$
φ	Activation function for processing element
Φ_m	Phase of mth harmonic IBC input, deg
$\Phi_m{}^*$	Φ_m/m, physical azimuth angle, deg
$\Delta\Phi_m$	Interval in Φ_m , deg
$\Delta\Phi_m{}^*$	Interval in $\Phi_m{}^*$, physical azimuth angle, deg
σ	Rotor solidity, $N_b c/\pi R$
ψ	Rotor azimuth angle, deg

Ω Rotor rotational speed

Introduction

Need for Neural Networks

The development and implementation of a robust active control system for helicopter aeromechanics must include an accurate representation of how the control inputs influence the measured outputs. A good example is how high frequency helicopter pitch inputs influence measured airframe vibration. For example, rotorcraft hub loads and vibration almost always behave nonlinearly with respect to the phase of a higher harmonic control (HHC) input. The following experimental and analytical work involving HHC highlights this problem: wind tunnel test results (Ref. 1); flight test results (Ref. 2); and analytical results (Ref. 3).

Neural network-based techniques are an attractive, nonlinear method for the modeling and prediction of nonlinear systems. Neural networks do not require large amounts of computational resources or central processor time. Additionally, compared to traditional methods they appear equally easy to apply and understand. Neural networks have not been extensively applied to problems in rotorcraft dynamics and the authors believe that the present study is the first of its kind.

A successful neural networks application enables the accurate nonlinear identification of important rotorcraft parameters. An efficient neural network application can enable the hardware implementation of feedback-driven control systems. In the present context, hardware implementation refers to the complete control system and its functions (which include modeling, optimizing, and controlling). Several nonlinear neural network modeler/optimizer/controller systems have been developed for industrial processes (Refs. 4 and 5).

Brief Survey of Existing Work

Haykin (Ref. 6) is an excellent reference for providing a practical understanding of neural networks. Narendra (Ref. 7) gives clear descriptions of two types of neural networks: back-propagation and radial-basis function, both of which are utilized in the current effort. Haas, Milano, and Flitter (Ref. 8) predicted helicopter component loads using neural networks that were based on flight test data. A back-propagation neural network was used in this study. Cabell, Fuller, and O'Brien (Ref. 9) applied neural networks to identify measured helicopter noise. A back-propagation neural network was used in that study.

The following is an overview of the present study. First, the topic of neural networks is introduced and descriptions are given of the types of neural networks that are used in the present effort. The experimental data sets used to develop neural networks are presented. Experimentally derived vibratory hub loads data, characterized by a single metric, form the single output of the neural network. The single input application is evaluated using four different data sets. The multiple input case is evaluated using one data set. Single input results include an investigation of the smallest number of training data pairs required to ultimately predict the global optimum phase. An error investigation is performed and directed towards deriving information of practical use (such as the minimum number of iterations required to obtain an acceptable network prediction). Results from a linear transfer matrix-based approach are compared with those from the nonlinear, neural network based approach. Additionally, a control-angle-interval-limit for the physical control angle is derived using the results of the neural networks.

Introduction to Neural Networks

Neural networks are nonlinear, iteratively adaptive methods of identification. The nonlinear feature becomes highly important if the underlying physical mechanism is inherently nonlinear (Ref. 6). Even when applied in a localized sense, linear methods (linear transfer matrix methods) may not be suitable for nonlinear systems.

Description of Typical Neural Networks

A neural network has one input layer, one output layer, and one or more hidden layers (Fig. 1, taken from Ref. 6). The input and output layers are made up of user-specified inputs and outputs. The hidden layers are comprised of nonlinear processing elements (PE's) which are described later.

The objective in developing a neural network (learning or training step) is to iteratively train the network using known, specified input data to minimize the error between the desired (known outputs) and the network outputs. Once this error (usually the RMS error) reaches an acceptably low level, the network is considered "trained", i.e., the modeling step is complete. The network can now be used to predict outputs at specified input values.

Figure 2 (taken from Ref. 6) shows a nonlinear model of an individual PE. Each hidden layer is made up of these PE's. The weights mulitiplying each individual input are initially unknown. The iterative adjustment of these weights, in order to reduce the RMS error in the network outputs, is the network design objective (training step). A user-specified activation function (transfer function), usually a hyperbolic tangent function, is implemented in the PE in order to control the output amplitude of the PE. Differentiable activation functions within each PE are preferable since some training algorithms use gradient information, such as the method of steepest descent.

Relevant Types of Neural Networks

Of the available networks, the following three were found to be useful in the present work:

1. Radial-Basis Function Neural Network (RBF Network)
2. General Regression Neural Network (GRNN)
3. Back-Propagation Neural Network

These networks are described below.

Radial-Basis Function Neural Network (RBF Network) Following the description of RBF networks given in Chapter 7 of Ref. 6, this approach views the design of neural networks as a curve-fitting (approximation) problem in a high-dimensional space. Learning is equivalent to finding a surface in a multidimensional space that provides the best fit to the training data. Network generalization (ability of the network to compute input-output relationships based on data never used in creating or training the network) is equivalent to the use of this multidimensional surface to interpolate training data. The formulation is based on traditional strict interpolation in a multidimensional space. In the context of a neural network, the hidden units provide a set of "functions" that constitute an arbitrary "basis" for the input patterns (vectors) when they are expanded into the hidden-unit space; these functions are called radial-basis functions. Radial-basis functions were first introduced in the solution of real multivariate interpolation problems and this topic is now one of the main fields of research in numerical analysis (Ref. 6).

A basic RBF network has one hidden layer. The hidden layer of a RBF network is nonlinear, whereas the output layer is linear. Gaussian functions are usually chosen as the radial-basis functions within the individual PE in the one hidden layer.

He and Lapedes (Ref. 10) introduced a second hidden layer into the basic RBF network. Compared to the basic, single, hidden layer RBF approach, this double hidden layer RBF approach involves successive approximations and is intended to result in reduced computation time and improved predictive ability.

He and Lapedes also introduced guidelines governing the selection of the RBF network size. In this paper, the authors extensively refer to these guidelines as He and Lapedes' guidelines. A description of these guidelines follows. If there are N pairs of input and output data available for training, then these N pairs can be partitioned into M groups where N is divisible by M. For example, in one of the applications in the present study there are 12 unique training (input) data pairs. This implies that there are 12 radial-basis centers available for each of the 12 pairs. Practically, in the two hidden layer formulation, there are 12 processing elements in the first hidden layer and any one of the following number of groups (M) in the second hidden layer : 6, 4, 3, or 2. Thus one possible

RBF network is: 1-12-6-1 where the first and last 1's refer to the number of inputs and outputs, respectively. Other possible RBF networks are: 1-12-4-1; 1-12-3-1; or 1-12-2-1. The present neural network application has a very small number of training data pairs compared to a typical neural network application that can have hundreds of training data pairs.

General Regression Neural Network (GRNN, Ref. 11)

GRNN is a general purpose paradigm network used primarily for system modeling and prediction and can be considered a generalization of a probabilistic neural network (Ref. 11). In addition to being used as a static regression technique, GRNN can be used in situations where the statistics of the data are changing over time. In the present effort GRNN was used in a limited manner. GRNN was used to provide a comparative benchmark for Case 3a, which is described later in the paper. A GRNN has one hidden layer.

Back-Propagation Neural Network

Back-propagation is the most popular neural network. This algorithm has two passes during the network design and training phase: the forward pass and a backward pass (Ref. 6). The forward pass produces network outputs in response to the inputs, with the weights being fixed during this pass. During the backward pass, the weights are adjusted to minimize a specified error criterion in accordance with an error correction rule. Specifically, network response (prediction) is subtracted from the desired (specified) response to produce an error signal. The error signal is then propagated backward through the network, against the direction of the connections, hence the name "error back-propagation" (Ref. 6).

A back-propagation neural network has two or more hidden layers. One of the applications in this study involves a trained back-propagation network with three hidden layers and 12 PE's in each hidden layer (1-12-12-12-1).

Present Application

The training data pairs that were used in this study were obtained from the second U.S./German Individual Blade Control wind tunnel test (IBC2 test). The test article was a four-bladed BO-105 hingeless rotor system (owned by NASA) fitted with German IBC electro-hydraulic actuators. The rotor system was tested in the NASA Ames 40- by 80-Foot Wind Tunnel (Refs. 12 and 13).

The five vibratory hub loads (axial force, side force, normal force, pitching moment, and rolling moment) obtained from the Rotor Test Apparatus steady/dynamic rotor balance in the fixed system were combined into a single metric (square root of the sum of the squares, with equal weighting). Only 4 per/rev (4P) load components were used. Data were acquired by a LabVIEW (Ref. 14) based data acquisition system. The single test condition used in this study is a simulated descent condition at an airspeed of approximately 65 knots (μ=0.15) and C_T/σ =0.075. Other test parameters are: α_s=2.9 deg, Ω=425 RPM, with the hub pitching and rolling moments trimmed to 1600 ft-lb and -350 ft-lb, respectively. This descent condition is equivalent to a 5.6 deg glide slope angle.

The mth harmonic IBC pitch input for the ith blade is defined as:

$$\theta_{im} = A_m \sin [m (\psi_i + 90 \text{ deg}) + \Phi_m]$$

This definition of the IBC phase Φ_m is the same as that used in the run logs for this test. This phase definition is different from the input phase angle definitions used in Refs. 12 and 13.

The relevant open loop control input sets are summarized in Table 1.

Input Set	Open Loop Control Mix of Inputs			
	A_2	Φ_2	A_3	Φ_3
A	1.0	0 to 360	0	0
B	0.5 to 2.0	210	0	0
C	0	0	0.5	0 to 360
D	1.0	210	0.5	0 to 360

Table 1. Range of relevant IBC open loop inputs

In the present application, the input layer in the neural network has one or four inputs:

i) 2P input phase (at fixed amplitude) or 2P input amplitude (at fixed input phase) - one input cases

ii) 2P and 3P input amplitudes and phases - four inputs case

The output layer has one output, the predicted vibratory hub loads metric. Detailed definitions of these cases follow.

Single Input, Single Output Cases

The following defines the one input, one output cases that were considered in this neural network study:

Case 1. Prediction of the vibratory hub loads metric versus the 2P phase (0 deg to 360 deg) with pitch control amplitude a constant 1 deg. Data were acquired at 30 deg intervals in the 2P phase input yielding 13 training data pairs ($\Delta\Phi_2$=30 deg). The first and last training pairs (Φ_2=0 deg and Φ_2=360 deg) have the same output metric. An interpolative type of prediction is involved in this case.

Case 2. Prediction of the vibratory hub loads metric for a known case with some data intentionally omitted in the network training phase. The region of interest is in the vicinity of the global minimum that occurs in the 2P phase variation of Case 1. The number of training data pairs is 12. An interpolative type of prediction (inbounds prediction) is involved in this case. The network's ability to generalize is studied in this case.

Case 3. Prediction of the vibratory hub loads metric with 2P control amplitude (A_2=0.5 deg to 2.0 deg) at a fixed input phase Φ_2=210 deg. This case has two sub-cases:

3a. Prediction at points which fall within the bounds of available experimental amplitude data. The number of training data pairs is four.

3b. Prediction at large amplitudes where experimental amplitude data are not available. This was done, again, by intentionally omitting data in the network training phase. This type of prediction is called an "out-of-bounds" prediction (extrapolation). The number of training data pairs is three.

Case 4. Prediction of the vibratory hub loads metric versus the 3P input phase (0 deg to 360 deg) with 3P pitch control amplitude A_3 a constant 0.5 deg. Data were acquired at 45 deg intervals in 3P phase yielding 9 training data pairs ($\Delta\Phi_3$=45 deg). The first and last training pairs (Φ_3=0 deg and Φ_3=360 deg) have the same output metric. An interpolative type of prediction is involved in this case.

Multiple Inputs, Single Output Case

The four inputs to the neural network in this application are:

1. 2P control amplitude, A_2
2. 2P control phase, Φ_2
3. 3P control amplitude, A_3
4. 3P control phase, Φ_3

A training data base with 37 pairs of input and output data was used. The composition of this 37-pair training data base is:

i) Thirteen data pairs for the vibratory hub loads metric's variation with 2P phase, A_2=1.0 deg, Φ_2=0 deg to 360 deg, and A_3=0 deg (same training data as in Case 1).

ii) Nine data pairs for the vibratory hub loads metric's variation with 3P phase, A_3=0.5 deg, Φ_3=0 deg to 360 deg, and A_2=0 (same training data as in Case 4).

iii) Nine data pairs for the vibratory hub loads metric's variation with 3P phase, A_3=0.5 deg, Φ_3 = 0 deg to 360 deg, with a superimposed 2P input given by A_2=1.0 deg, Φ_2 = 210 deg.

iv) Four data pairs for the absolute baseline metric (zero 2P and 3P amplitudes).

v) Two data pairs for the baseline metric in the presence of the following 2P input: A_2=1.0 deg, Φ_2 = 210 deg.

Baseline Training Data The baseline metric in Item iv) is associated with zero 2P and 3P amplitudes and is valid for all values of the 2P and 3P phase in the domain of interest. In the present application, this baseline metric value shows up as a horizontal line when plotted versus phase (0 deg to 360 deg). The inputs that constitute the four-pair training data formulation for the baseline in Item iv) is thus:

	A_2	Φ_2	A_3	Φ_3
1.	0	0	0	0
2.	0	360	0	0
3.	0	0	0	360
4.	0	360	0	360

These four training inputs are associated with four identical baseline values for the vibratory hub loads metric. Similar considerations hold for the 2-pair baseline formulation in Item v).

Results

The application of neural networks was conducted using NeuralWorks Pro II/PLUS (version 5.2) neural networks package by NeuralWare (Ref. 11). The Pro II/PLUS package was installed on an ACER Acros personal computer with an Intel 486DX2/66 central processor. All network applications in this study required approximately one to two minutes of clock time to complete the training step. Network prediction of an output case took less than one second, even for the multiple inputs case.

Single Input, Single Output Application

Case 1. Metric Versus 2P Control Phase Input

Figure 3 shows the metric's nonlinear variation with 2P control phase (A_2=1 deg) from the IBC2 test. The baseline value is the vibratory hub loads metric without any IBC inputs. Two local minima were identified/measured during the wind tunnel testing.

All three types of neural networks noted earlier were considered (RBF, GRNN, and back-propagation). Of these three networks, an RBF network with two hidden layers gave the best results for this case. In this paper, only RBF networks with two hidden layers are studied. The first hidden layer uses Gaussian functions in the PE's. The second hidden layer and the output layer always use hyperbolic tangent functions in the PE's, unless otherwise noted. Thus, all RBF networks used in this study have a nonlinear output layer which is unlike a basic RBF network.

Several RBF networks with varying numbers of PE's in the hidden layers were studied. The first successful RBF network in this sequence of attempts is described as follows.

1-20-15-1 RBF Network This RBF network has one input, 20 PE's in the first hidden layer, 15 PE's in the second hidden layer, and one output. Network training for the 1-20-15-1 RBF network was terminated after 5646 iterations; the final RMS error was 0.0041. The resulting network predictions are shown in Fig. 4. The figure shows the trained network outputs as open triangles at the training data points. This comparison shows the success of the training process (modeling) to match the experimental data set.

Also shown in Fig. 4 are predicted outputs (interpolated outputs) from the network at intermediate points for which there are no experimentally-derived metric data available. Figure 4 shows that the 1-20-15-1 RBF network can be used to model and predict the nonlinear variation of the metric with 2P control phase.

Figure 4 also shows the curve fit from a linear, single harmonic transfer matrix approach. The linear results were obtained from the linear regression analysis routines available in Ref. 14. This linear harmonic fit represents the technology currently used in helicopter vibration control studies such as Ref. 15. The nonlinear neural network fit is clearly more accurate. The neural network predicts the optimum phase in the vicinity of 255 deg. The linear transfer matrix identifies a global optimum around 230 deg.

Revised Radial-Basis Function Networks When a neural network learns too many specific input-output relations, the

network is overtrained. The network may memorize the training data and be less able to generalize. Also, if more than the necessary PE's are used in forming a network, then unintended curves in the problem space are stored in the network weights (Ref. 6). Therefore, the 1-20-15-1 RBF network was revised to preclude invalid function approximations which can result in grossly incorrect predictions.

The revised RBF networks are based on the He and Lapedes' guidelines. With 13 training data pairs available for training, a 1-12-4-1 RBF network was investigated.

The 1-12-4-1 RBF network was trained for 10,000 iterations; the final RMS error was 0.0039. The resulting modeling and prediction are shown in Fig. 5. Clearly (Figs. 4 and 5), the 1-12-4-1 RBF network performs just as well as the 1-20-15-1 RBF network. For both networks, a global minimum vibratory hub loads metric value is predicted at a 2P phase control angle of 255 deg, although the 1-12-4-1 RBF network predicts a 10 percent lower metric value at Φ_2=255 deg. The 1-12-4-1 RBF network can also be used to model and predict the nonlinear variation of the metric with 2P phase.

Table 2 shows that the two trained networks had similar clock times.

RBF Network	No. of Iterations	RMS error	Clock time seconds
1-20-15-1	5646	0.0039	60
1-12-4-1	10,000	0.0041	70

Table 2. Comparison of clock times for two RBF networks

Error Investigation An error investigation was conducted in order to determine the acceptable RMS error level while maintaining an acceptable curve fit. Figure 6 shows a comparison of the RMS error variations for four RBF networks up to 10,000 iterations. These networks follow the He and Lapedes' guidelines and are given by: 1-12-4-1; 1-12-6-1; 1-12-3-1; and 1-12-2-1. The RMS error variations for the latter two RBF networks, 1-12-3-1 and 1-12-2-1, are indistinguishable from one another in Fig. 6. The comparison in Fig. 6 shows that depending on the acceptable error level, one could work with any one of the four networks. For present purposes, the 1-12-4-1 RBF network which had the smallest error at 10,000 iterations is taken as the baseline network for further study.

Figure 7 shows the curve fits obtained from the baseline 1-12-4-1 RBF network for various error levels, or equivalently, number of iterations. The RMS error ranges from approximately 0.01 (6772 iterations) to 0.10 (1104 iterations). Figure 7 shows that each of the four curve fits follows the general shape of the training "curve". To investigate the RBF network's behavior around the metric's minimum value region, the predicted metric is shown Fig. 8 for a focused phase space (120 deg to 360 deg). The results shown in Fig. 8 suggest that approximately 1100 training iterations are sufficient to predict the vibratory hub loads metric in the neighborhood of the global minimum and more importantly, to ultimately predict the optimum phase. In this case, the 1100 training iterations were performed in less than 10 seconds of clock time.

Case 2. Missing Data Prediction
In order to determine whether a 1-12-4-1 RBF network can predict the vibratory hub loads metric's global minimum with the 270 deg training data pair omitted, a new 1-12-4-1 RBF network was trained. This new 1-12-4-1 RBF network used 12 training data pairs. Figure 9 shows the resulting interpolation, inbound prediction. The 1-12-4-1 RBF network is successfully used to predict the global minimum and optimum phase in the vicinity of missing data.

Case 3. Metric Versus 2P Control Amplitude
This case involves variation in the vibratory hub loads metric with 2P control amplitude A_2 at a fixed 2P phase Φ_2=210 deg. This case involves two sub-cases: inbound sub-case (Case 3a); and an out-of-bounds sub-case (Case 3b). The respective number of available training data pairs for training are four (inbound and out-of-bounds) and three (out-of-bounds). Results

from the RBF, GRNN, and back-propagation networks are presented.

Predictions by RBF Network

Case 3a Figure 10 shows the results using a 1-4-2-1 RBF network. The network was trained for 4000 iterations; the final RMS error was 0.0000. The inbound prediction (interpolation) is acceptable. Any potential rate of increase of the vibratory hub loads metric in the out-of-bounds region ($A_2 > 2$ deg) is not captured by the RBF network. This may be an inherent characteristic of RBF networks due to their interpolative basis preventing satisfactory extrapolation.

Case 3b Figure 11 shows the results from a 1-3-1-1 RBF network. Recall Case 3b uses the same training pairs as Case 3a except the A_2=2 deg data point is excluded. The network was trained for 4000 iterations; the final RMS error was 0.0000. Figure 11 shows an unacceptable out-of-bounds prediction; the actual data at A_2=2 deg (extrapolation) is not predicted. An RBF network with linear transfer functions in the second hidden and output layers was also designed with no prediction improvement. The vibratory hub loads metric's drop-off in the out-of-bounds region persisted even with the use of the linear transfer function PEs. The unacceptable extrapolation resulting from the RBF network led to additional studies involving other neural networks.

Prediction by GRNN

Case 3a Figure 12 shows shows the results for this sub-case using a 1-20-1 GRNN. The network was trained for 1000 iterations; the final RMS error was 0.0172. The attributes of this network were defined by the default options for this type of network (Ref. 11). The inbound prediction (interpolation) is again acceptable whereas the out-of-bounds prediction (extrapolation) is unacceptable as the network experiences "turn-off" beyond the training data base.

Prediction by Back-Propagation Network

Case 3a Figure 13a shows the prediction from a 1-12-12-12-1 back-propagation network. The hyperbolic tangent transfer function was selected for all layers in the network. The network was trained for 4000 iterations; the final RMS error was 0.0039. The inbound prediction is again acceptable. However, this network also demonstrates a moderate "turn-off" characteristic beyond the training base ($A_2 > 2.0$ deg).

Figure 13b shows results for the same case, Case 3a, with a linear transfer function PE selected for the back-propagation network's output layer and maintaining hyperbolic tangent function PE's for the three hidden layers. The RMS error for this network was 0.0018, with all other network parameters unchanged. Figure 13b shows that there is no "turn-off" phenomenon in the extrapolation beyond the training base for this back-propagation network.

Case 3b Figure 14a shows the results from a 1-12-12-12-1 back-propagation network. The hyperbolic tangent transfer function was selected for all network layers. The network was trained for 4000 iterations; the final RMS error was 0.0000. The extrapolation is unacceptable.

Figure 14b shows results for the same case, Case 3b, with linear transfer function PE's selected for all layers of the 1-12-12-12-1 back-propagation network. This network was trained for 4000 iterations; the final RMS error was 0.0361. Figure 14b shows acceptable extrapolation. The success of the back-propagation network compared to the RBF network and GRNN in extrapolation may be the result of the experimental data being approximately linear with amplitude. Thus, one observation is that the back-propagation network is able to extrapolate provided the network is given guidance on the basic behavior of the plant model, i.e., the extent of linearity present in the system.

Case 4. Metric Versus 3P Control Phase Input

The measured vibratory hub loads loads metric variation with a 3P control phase input (at a constant amplitude A_3=0.5 deg) is shown in Fig. 15. The training data have one minimum, the global minimum, within the first quadrant. There are nine training data pairs available (45 deg intervals), and applying the He and Lapedes' guidelines, the selected RBF network is 1-9-3-

1. Network training was terminated after 6000 iterations and the final RMS error was 0.0169. These results (Fig. 15) show that the 1-9-3-1 RBF network successfully models and predicts the nonlinear variation of the vibratory hub loads metric with 3P input phase. Figure 15 also shows the acceptable linear fit for this case with one minimum in the vibratory hub loads metric variation. This valid fit in optimum control phase angle is expected since a single harmonic is being used in the linear approach. The actual vibratory hub loads metric at the minimum is overpredicted, however, by over 20 percent.

In contrast to the good prediction shown in Fig. 15, Fig. 16 shows a bad prediction for Case 4 based on a 1-20-15-1 RBF network which does not follow He and Lapedes' guidelines. This network was trained for 6000 iterations; the final RMS error was 0.0004. This figure shows a shortcoming in overspecifying a network to achieve a very small RMS error. The 1-20-15-1 network yields poor inbound predictions within certain input phase angle intervals.

Multiple Inputs, Single Output Application

In the present study, RBF networks have been successful in the one input, one output applications covered under Cases 1, 2, and 4. These three cases involved interpolation, or inbound prediction. The four inputs, one output application of neural networks presented here also used an RBF network with Gaussian functions in the first hidden layer, and hyperbolic tangent functions in the second hidden layer and the output layer.

Following the He and Lapedes' guidelines as applied to the presently formulated 37-pair training data base, a 4-36-9-1 RBF network was used. The 4-36-9-1 RBF network was trained for 10,000 iterations; the final RMS error was 0.0205. As an indication of the success of the training, Fig. 17 shows the 37 predicted outputs versus the corresponding desired outputs (measured training data). The modeling step was successful. Figure 18 shows the RMS error variation with the number of iterations. A better model may be achieved by increasing the number of training iterations; however, this is probably not necessary for engineering purposes.

The predictions from the trained 4-36-9-1 RBF network are shown in Fig. 19. Figure 19a shows acceptable prediction of the vibratory hub loads metric as obtained from the 4-36-9-1 RBF network for the interpolative case when 2P control phase is the input (at a constant amplitude A_2=1.0 deg). The accompanying baseline metric's prediction (no IBC input, $A_2 = A_3$=0 deg) is also acceptable. The corresponding single-input prediction (Case 1) was shown in Fig. 5.

Figure 19b shows acceptable prediction of the vibratory hub loads metric as obtained from the 4-36-9-1 RBF network for the interpolative case when 3P control phase is the input (at a constant A_3=0.5 deg). The accompanying baseline metric's prediction (no IBC input, $A_2 = A_3$=0 deg) is also acceptable. The corresponding single-input prediction (Case 4) was shown in Fig. 15.

Figure 19c shows acceptable prediction for the vibratory hub loads metric as obtained from the 4-36-9-1 RBF network for the interpolative case when 3P control phase is the input (at a constant A_3=0.5 deg, and A_2=1.0 deg and Φ_2=210 deg). The accompanying baseline metric's prediction (with IBC input, A_2=1.0 deg and Φ_2=210 deg, A_3=0) is also acceptable.

For this particular network training, the two baselines were cast as 4-pair and 2-pair training data bases, respectively. Figures 19a to 19c show that the RBF network baseline predictions are not strictly linear. The authors believe that this prediction can be improved by specifying a finer resolution in the phase space associated with the training data for the baselines. Depending on a user specified band of tolerance for the modeling of the baseline vibratory hub loads metric, one could specify information regarding the baseline metric at, for example, 60 deg intervals instead of the present 360 deg interval. However, an increase in the resolution of this "baseline" phase space will increase the size of the overall training data base, and will consequently increase the clock time required for completion of the training step.

Nevertheless, the 4-36-9-1 RBF network can be used to model and interpolatively predict the nonlinear vibratory hub loads metric when there are four inputs (2P and 3P amplitudes and phases).

Considerations for Neural Network Application and Feedback Control

An efficient neural network application can enable accurate plant modeling control system feedback. In the present context, an efficient neural network application is defined as one that can successfully perform plant model identification using a minimum number of training data pairs. The acquisition of training data (and subsequent network learning) can require considerable time. Reducing the number of required training data pairs can reduce the time both in data acquisition and in network design calculation. Additionally, in many instances such as vibratory hub loads control, the potential number of training pairs for all input control combinations, including amplitude and phase variations, result in situations where the training base will only be a small portion of the possible control input combinations that make up the complete data set.

In Case 1, the number of available training data pairs was 13 ($\Delta\Phi_2$=30 deg phase interval). The following four figures show predictions from four different RBF networks using training data at $\Delta\Phi_2$=60 deg and $\Delta\Phi_2$=90 deg phase intervals. Note that this selection of training pairs results in the 0 deg and 360 deg pairs being omitted from the training base. In order to maintain periodicity in each of these four cases, the 0 deg and 360 deg training pairs were always included. Depending on which interval ($\Delta\Phi_2$=60 deg or 90 deg) is under consideration, the actual number of training pairs used in training the network thus turns out to be one of the following: 7, 8, 5, or 6 (Figs. 20, 21, 22, and 23, respectively). All four RBF networks used He and Lapedes' guidelines and were trained for 10,000 iterations. These figures also contain results from the linear transfer matrix approach using the exact same input data base as that used by the corresponding RBF network.

Figures 20 and 21 show predictions from two RBF networks (1-6-3-1 and 1-8-4-1) that used different $\Delta\Phi_2$=60 deg phase interval training data bases. Figure 20 shows results from a 7-pair 1-6-3-1 RBF network trained with data pairs at the following phase values: Φ_2=0, 60, 120, 180, 240, 300, and 360 deg. This network had a final RMS error of 0.0160. Although not capturing the nonlinear behavior (local maxima) at Φ_2=210 deg, the global minimum is predicted very well (Φ_2=270 deg). Figure 21 shows results from the 8-pair 1-8-4-1 RBF network trained with data pairs at the following phase values: Φ_2=0, 30, 90, 150, 210, 270, 330, and 360 deg. This network had a final RMS error of 0.0003. Here the nonlinear behavior at Φ_2=210 deg is modeled yet the global minimum is predicted to be at Φ_2=285 deg. Nevertheless, clearly the 1-6-3-1 and 1-8-4-1 RBF networks using a $\Delta\Phi_2$=60 deg phase interval data base can be successfully used to model and predict the nonlinear variation of the vibratory hub loads metric with 2P control phase. Global minima are well predicted. The results from the linear single harmonic transfer matrix approach are not as accurate as the results from the neural network approach. In both cases the linear transfer matrix gives a global minimum around Φ_2=230 deg.

Figures 22 and 23 show the curve fits from two RBF networks (1-4-2-1 and 1-6-3-1) that used different $\Delta\Phi_2$=90 deg phase interval training data bases. Figure 22 shows results from the 5-pair 1-4-2-1 RBF network trained with data pairs at the following phase values: Φ_2=0, 90, 180, 270, and 360 deg. The final RMS error was 0.0000. Similar to Fig. 22, Fig. 23 shows results from the 6-pair 1-6-3-1 RBF network trained with the data pairs at the following phase values: Φ_2=0, 60, 150, 240, 330, and 360. The final RMS error was 0.0112. Considering that the global minimum for the Case 1 vibratory hub loads metric's variation exists in the vicinity of 270 deg, it can be seen from Figs. 22 and 23 that this minimum is not well predicted by the 1-4-2-1 and 1-6-3-1 RBF networks using a $\Delta\Phi_2$=90 deg phase interval data base. The linear transfer matrix predictions are even worse for both cases.

Largest Acceptable Phase Interval The actual rotor azimuth phase intervals involved in the interpolative type of predictions that have been presented so far in this paper can be summarized as:

Case No., nP	Training Data	Azimuth Interval# $\Delta\Phi_n^*$	Prediction (RBF network)
1, 2P	13-pair	15	Acceptable
2, 2P	12-pair	15	Acceptable
4, 3P	9-pair	15	Acceptable
1, 2P	7-,8-pair	30	Acceptable
1, 2P	5-,6-pair	45	Unacceptable

deg, for nP control input $\Delta\Phi_n^*=\Delta\Phi_n/n$, physical rotor azimuth control interval

It appears that for an acceptable prediction, $\Delta\Phi_n^*=30$ deg is the largest rotor azimuth phase interval that can be tolerated (control-angle-interval-limit). The nonlinear vibratory hub loads metric's trend and the control-angle-interval-limit may be determined by the physics of the basic phenomenon that is important during the experimental test condition (in this case a simulated descent). Here the rotor vibratory loading is due in large part to blade vortex interaction. Further studies are obviously required on this subject. However, for this study, the maximum allowable phase interval for data training is $\Delta\Phi_n^*=30$ deg.

Conclusions

This paper presents an application of neural networks involving the nonlinear modeling and prediction of measured rotorcraft hub loads as represented by a single vibratory hub loads metric. The authors believe that this application is the first of its kind. Using 2P and 3P control input phase or amplitude as network input, the vibratory hub loads metric is the network output. The results from the present study show that neural networks accurately model experimental data. Issues in implementing a feedback control system using a linear transfer matrix approach versus a neural network approach were studied. Specific findings include:

1. The radial-basis function (RBF) neural network works well when 2P or 3P phase is the network input (at constant control input amplitude). The RBF network is robust for interpolation purposes, including significant nonlinearities.

2. The back-propagation neural network works well when 2P control amplitude is the network input (at constant control phase). The back-propagation network is also robust for interpolation purposes. For the data set studied, acceptable predictions for extrapolation purposes are produced.

3. RBF neural networks are superior to linear transfer matrix plant models for the experimental vibratory hub loads data presented in this paper, particularly 2P IBC data.

4. The smallest number of RBF network training data pairs, i.e., that which results in the most efficient network, depends on a newly identified interval limit for the physical azimuth control angle. This control-angle-interval-limit, $\Delta\Phi^*=30$ deg, is believed to be linked to the basic physical phenomenon that is important at the present experimental test condition, namely, the blade vortex interaction phenomenon.

5. The RBF neural network works well when there are multiple inputs to the network (2P and 3P control amplitudes and phases) and prediction is of the interpolative type. This includes predictions of the significantly nonlinear, non-baseline metrics and the accompanying baseline metrics.

References

1. Kottapalli, S., Swanson, S., LeMasurier, P., and Wang, J., "Full-Scale Higher Harmonic Control Research to Reduce Hub Loads and Noise," 49th Annual Forum of the American Helicopter Society, St. Louis, Missouri, May 1993.

2. Miao, J., Kottapalli, S.B.R., and Frye, H.M., "Flight Demonstration of Higher Harmonic Control (HHC) on S-76," 42nd

Annual Forum of the American Helicopter Society, Washington, D.C., June 1986.

3. O'Leary, J.J., Kottapalli, S.B.R., and Davis, M., "Adaptation of a Modern Medium Helicopter (Sikorsky S-76) to Higher Harmonic Control," 2nd Decennial Specialists Meeting on Rotorcraft Dynamics, NASA Ames Research Center, Moffett Field, California, November 1984.

4 Graettinger, T.M., Bhat, N.V., and Buck, J.S., "Adaptive Control with NeuCOP, the Neural Control and Optimization Package," IEEE International Conference on Neural Networks, 1994.

5. Graettinger, T.M., Bhat, N.V., Heckerdorn, K., and Buck, J.S., "Model Predictive Control Using Neural Networks," The AIChE 1994 Spring National Meeting; Advances in Process Operations: Industrial Success Stories, April 1994 .

6. Haykin, S., Neural Networks, A Comprehensive Foundation, Macmillan, New York, 1994.

7. Narendra, K.S.,"Adaptive Control of Dynamical Systems Using Neural Networks," Handbook of Intelligent Control, Edited by D. A. White and D.A. Sofge, Van Nostrand Reinhold, New York, 1992.

8. Haas, D.J., Milano, J., and Flitter, L., "Prediction of Helicopter Component Loads Using Neural Networks," Journal of the American Helicopter Society, Vol. 40, No. 1, January 1995.

9. Cabell, R.H., Fuller, C.R., and O'Brien, W.F., "A Neural Network for the Identification of Measured Helicopter Noise," Journal of the American Helicopter Society, Vol. 38, No. 3, July 1993.

10. He, X. and Lapedes, A., "Nonlinear Modeling and Prediction by Successive Approximation Using Radial Basis Functions," Physica D 70, 1993.

11. NeuralWorks Manuals:
    a. Reference Guide
    b. Neural Computing
    c. Using NeuralWorks
    NeuralWare, Inc., Pittsburgh, Pennsylvania, 1995.

12. Jacklin, S., Blaas, A., Kube, R., and Teves, D., "Reduction of Helicopter BVI Noise, Vibration, and Power Consumption through Individual Blade Control," 51st Annual Forum of the American Helicopter Society, Ft. Worth, Texas, May 1995.

13. Swanson, S. M., Jacklin, S., Blaas, A., Niesl, and Kube, R., "Acoustics Results from a Full-Scale Wind Tunnel Test Evaluating Individual Blade Control," 51st Annual Forum of the American Helicopter Society, Ft. Worth, Texas, May 1995.

14. LabVIEW Manuals:
    a. User Manual for Windows
    b. Analysis VI Reference Manual
    National Instruments Corporation, Austin, Texas, September 1994.

15. Welsh, W., Fredrickson, C., Rauch, C., and Lyndon, I., "Flight Test of an Active Vibration Control System on the UH-60 Black Hawk Helicopter," 51st Annual Forum of the American Helicopter Society, Fort Worth, Texas, May 1995.

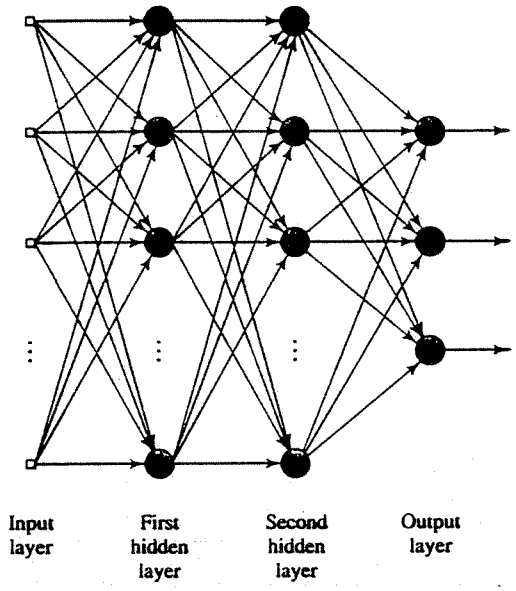

Fig. 1 Multi-Layered Neural Network (Ref. 6)

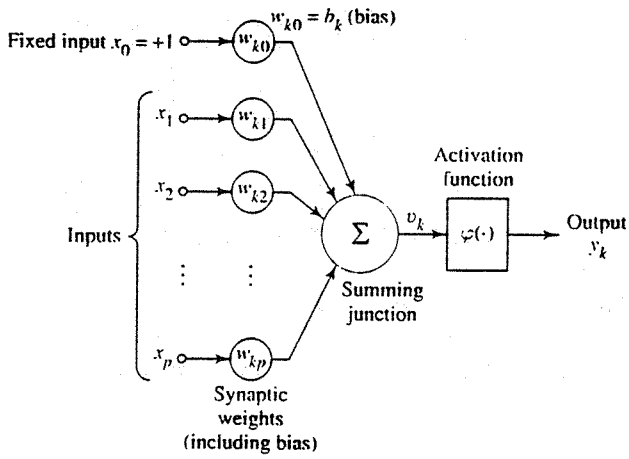

Fig. 2 Nonlinear model of a processing element (Ref. 6)

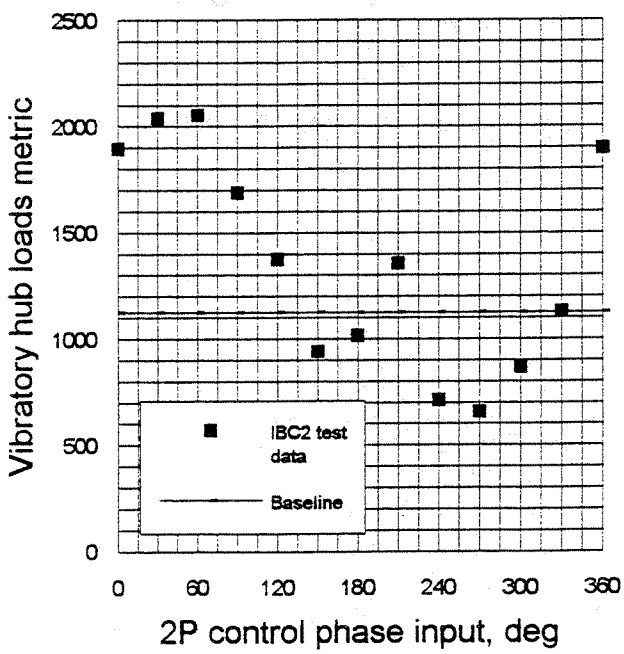

Fig. 3 Experimentally-derived nonlinear vibratory hub loads metric versus 2P control phase input, Φ_2

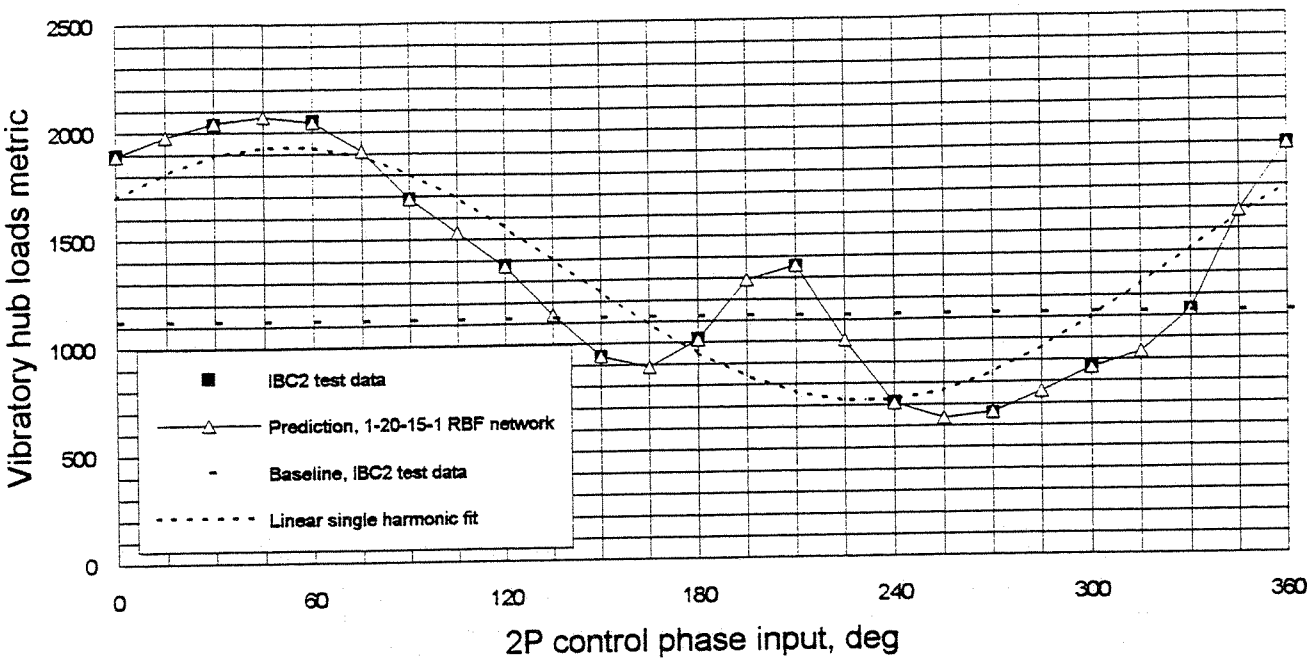

Fig. 4 Case 1: 1-20-15-1 Radial-Basis Function (RBF) neural network modeling and prediction of vibratory hub loads metric, variation with 2P control phase, Φ_2 (A_2=1.0 deg)

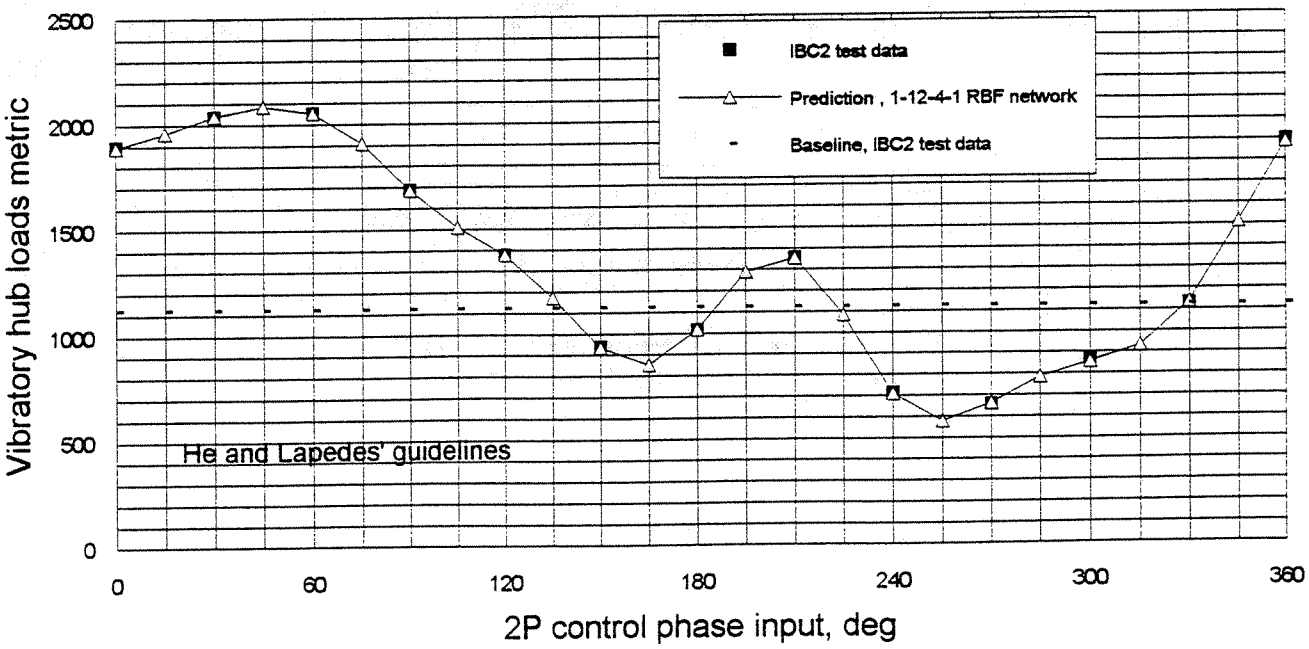

Fig. 5 Case 1: 1-12-4-1 RBF neural network modeling and prediction of vibratory hub loads metric, variation with 2P control phase, Φ_2 (A_2=1.0 deg)

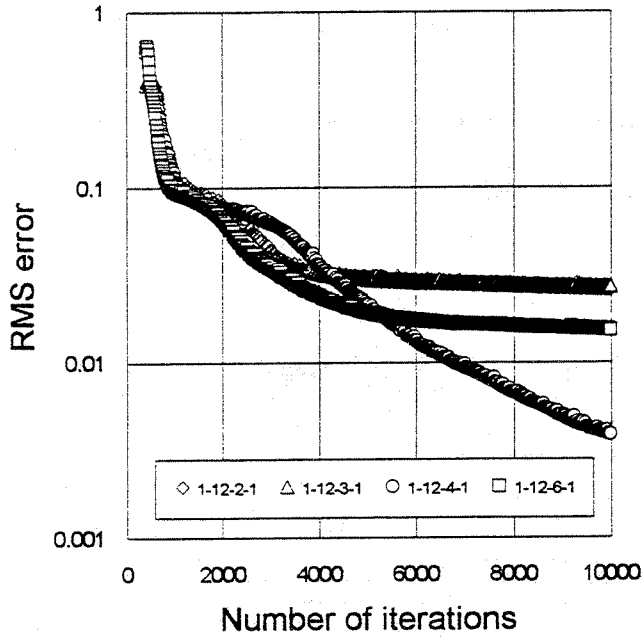

Fig.6 Case 1: Comparison of RMS errors for four RBF networks

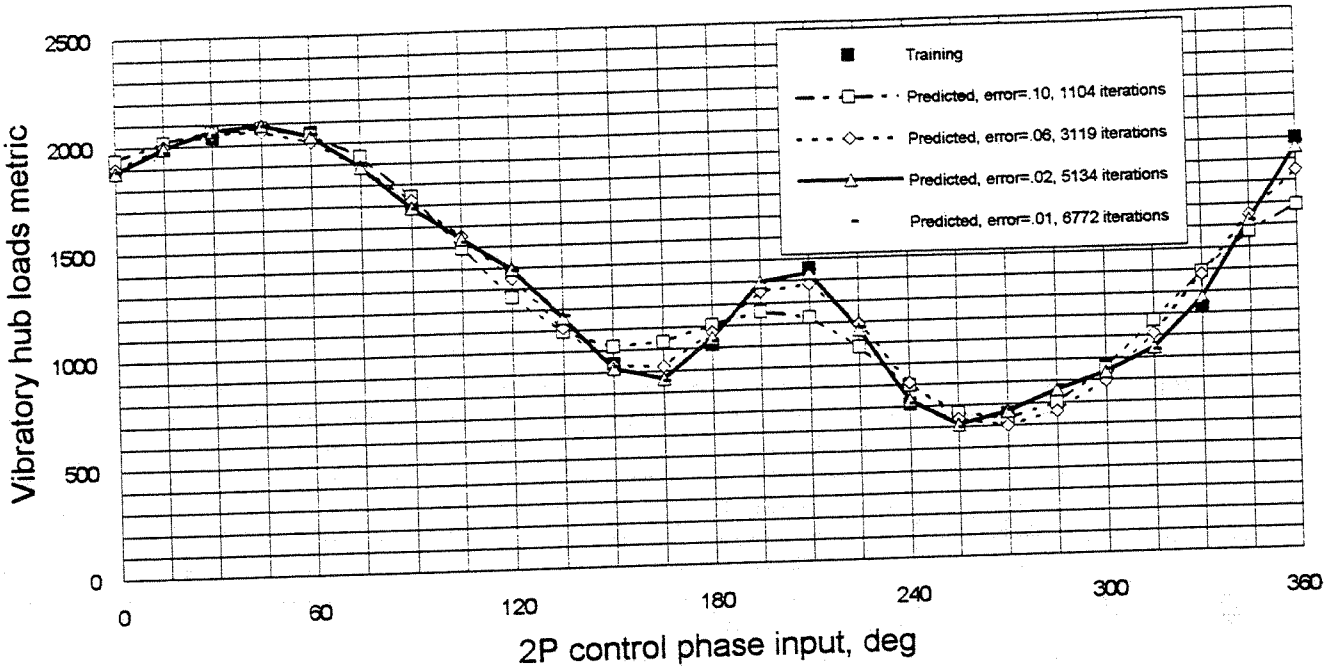

Fig. 7 Case 1: 1-12-4-1 RBF network modeling and prediction for varying RMS error levels (equivalently, number of iterations)

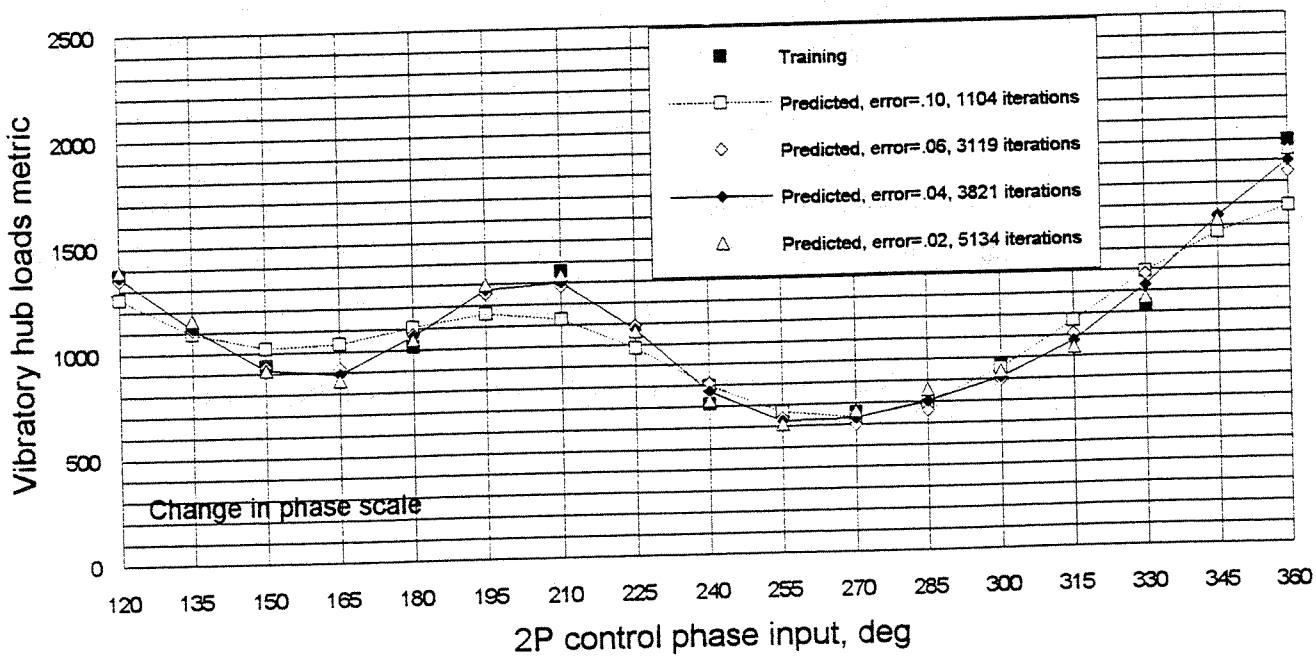

Fig. 8 Case 1: 1-12-4-1 RBF network modeling and prediction for varying RMS error levels (equivalently, number of iterations), focused scale (Φ_2=120 deg to 360 deg)

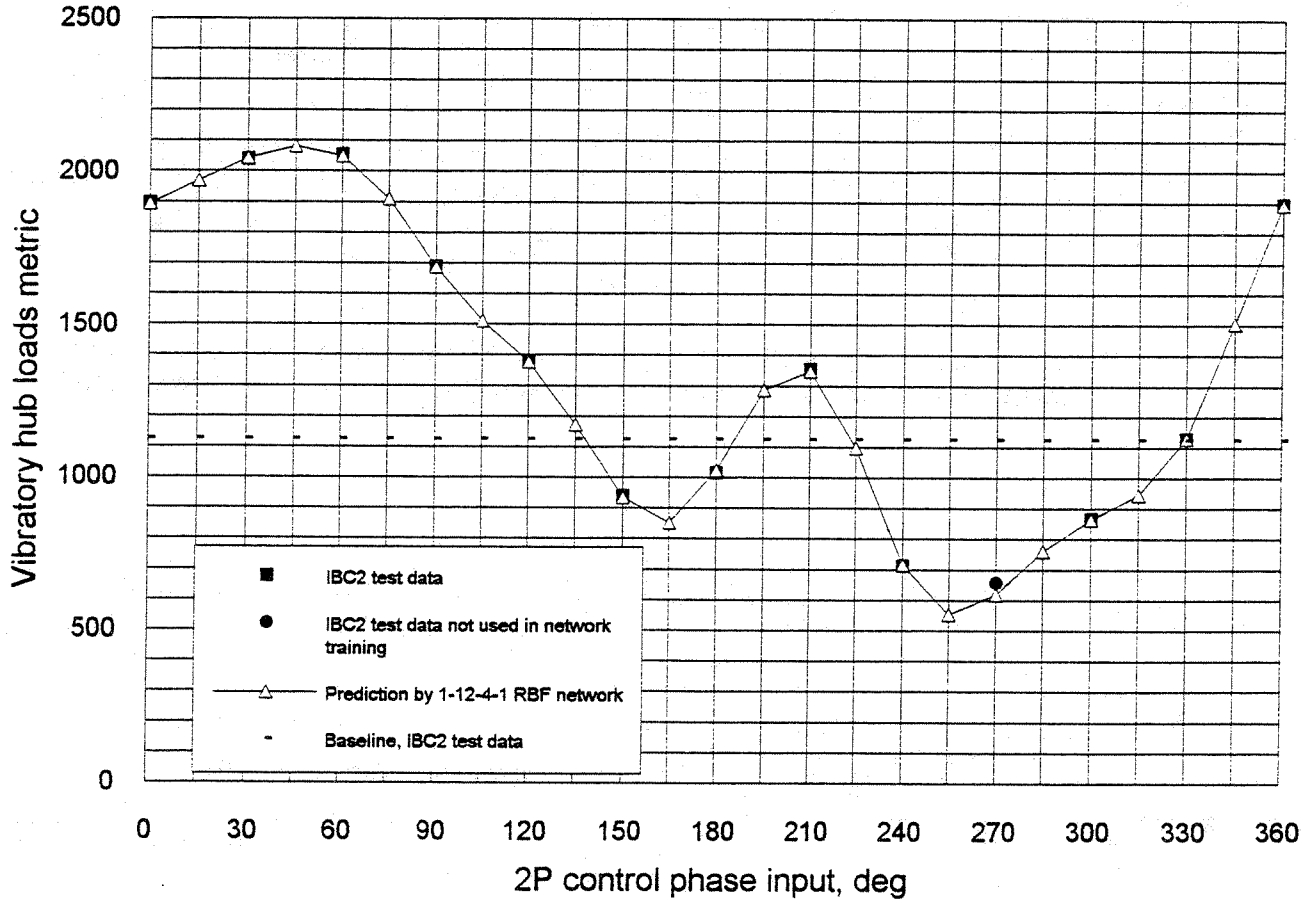

Fig. 9 Case 2: 1-12-4-1 RBF network, missing data modeling and prediction

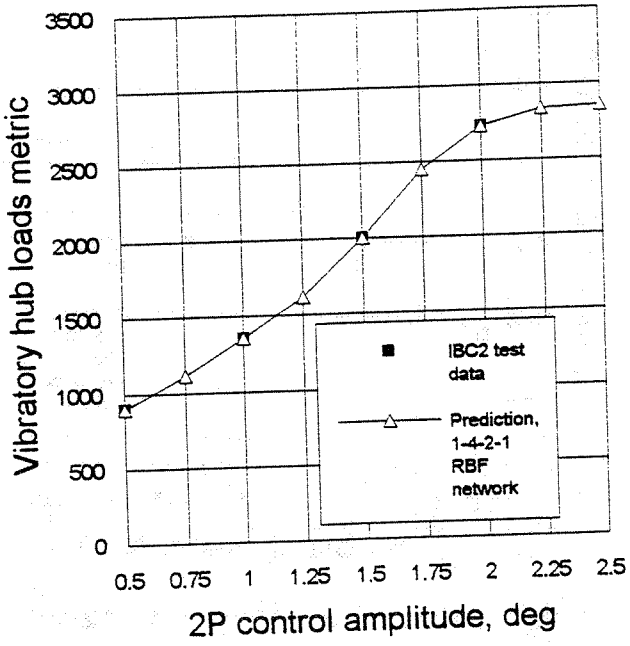

Fig. 10 Case 3a: 1-4-2-1 RBF network modeling and prediction, inbound prediction (interpolation)

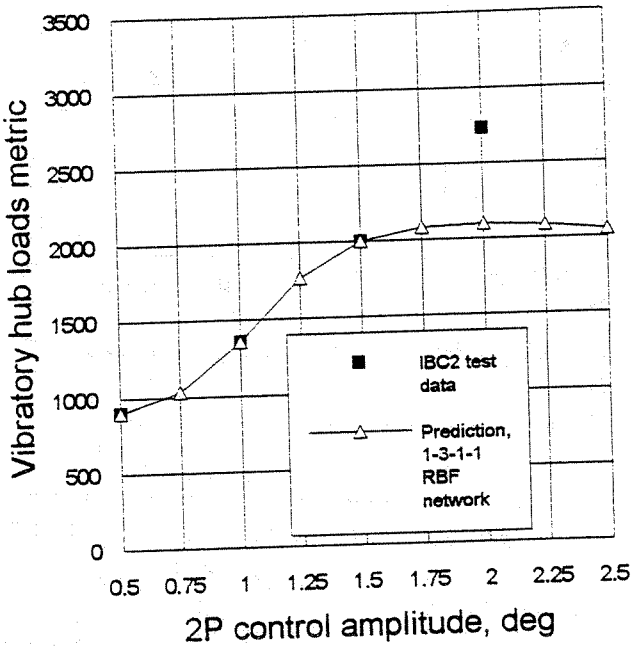

Fig. 11 Case 3b: 1-3-1-1 RBF network modeling and prediction, out-of-bounds prediction (extrapolation)

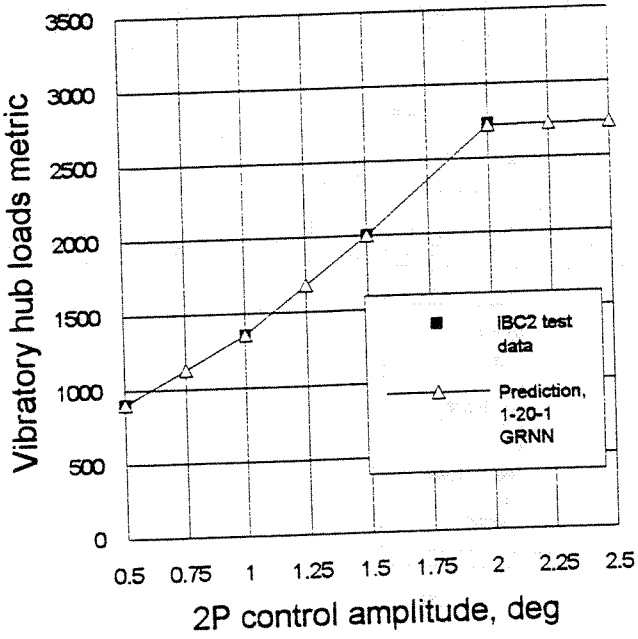

Fig. 12 Case 3a: 1-20-1 GRNN modeling and prediction, inbound prediction (interpolation)

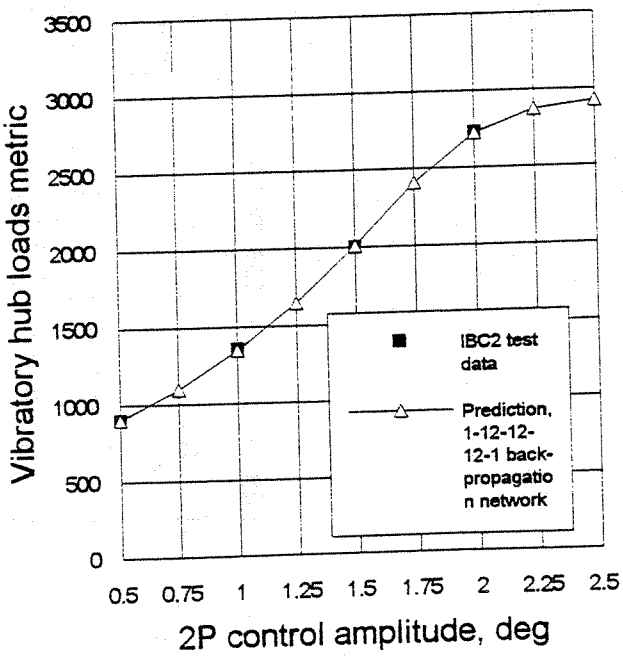

Fig. 13a Case 3a: 1-12-12-12-1 back-propagation network, hyperbolic tangent transfer function for all layers, inbound prediction (interpolation)

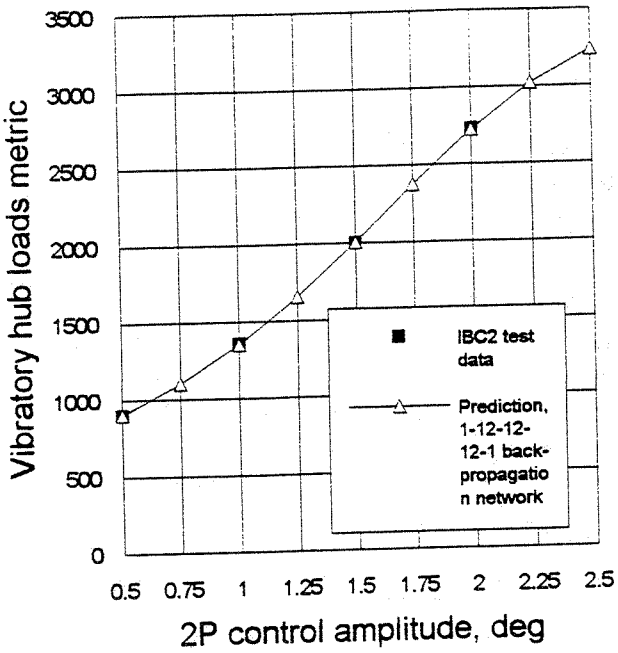

Fig. 13b Case 3a: 1-12-12-12-1 back-propagation network, linear transfer function for output layer,inbound prediction (interpolation)

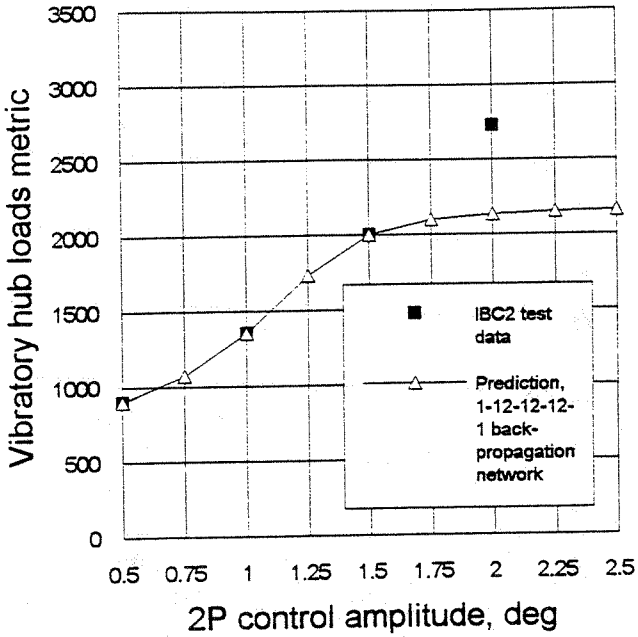

Fig. 14a Case 3b: 1-12-12-12-1 back-propagation network, hyperbolic tangent transfer function for all layers,out-of-bounds prediction (extrapolation)

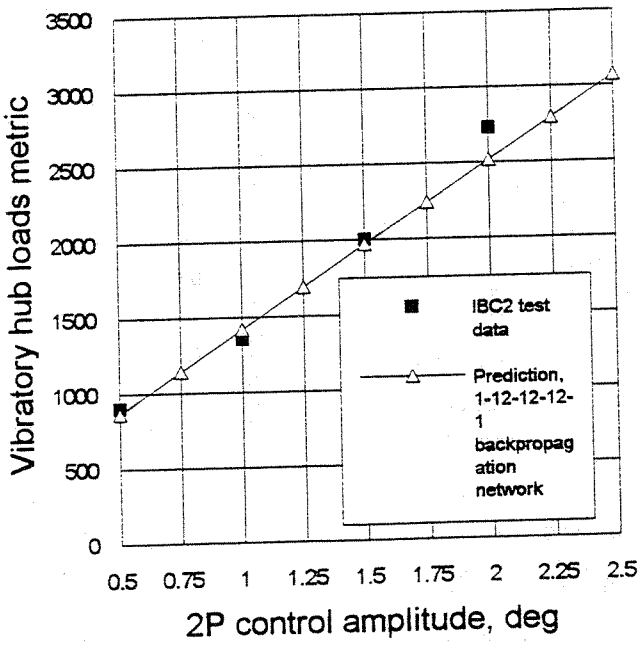

Fig. 14b Case 3b: 1-12-12-12-1 back-propagation network, linear transfer functionfor all layers,out-of-bounds prediction (extrapolation)

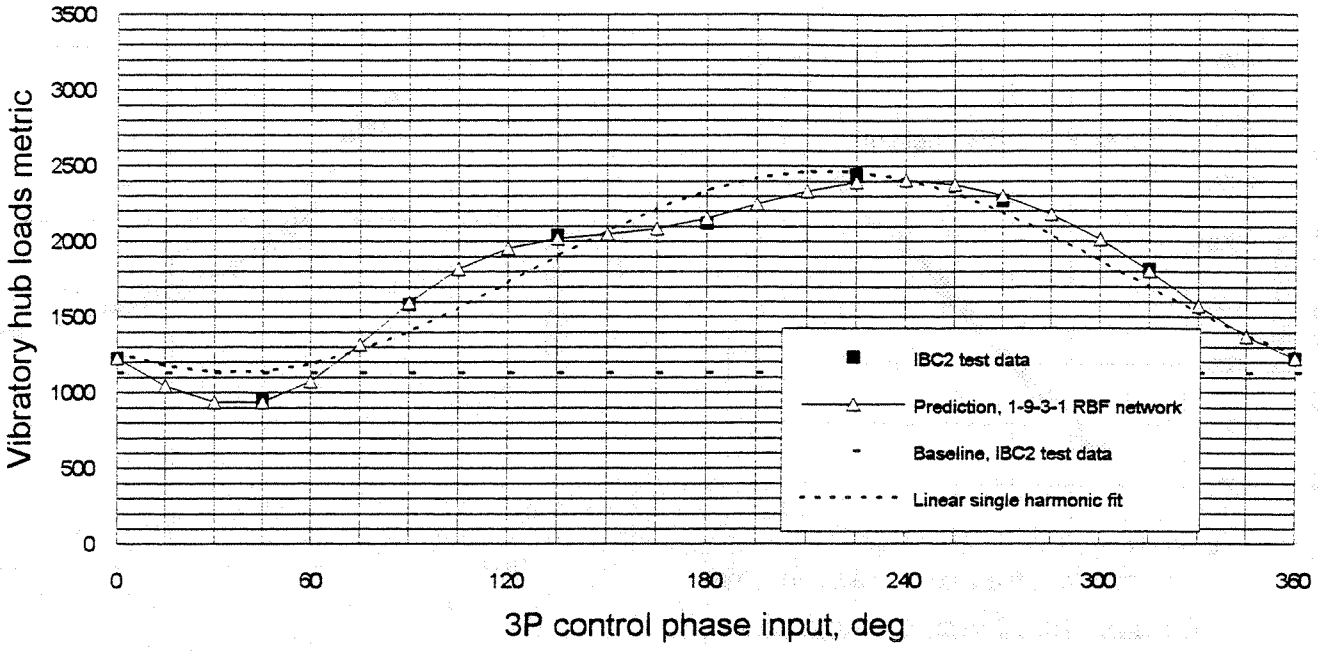

Fig. 15 Case 4: 1-9-3-1 RBF neural network modeling and prediction of vibratory hub loads metric, variation with 3P phase, Φ_3 (A_3=0.5 deg)

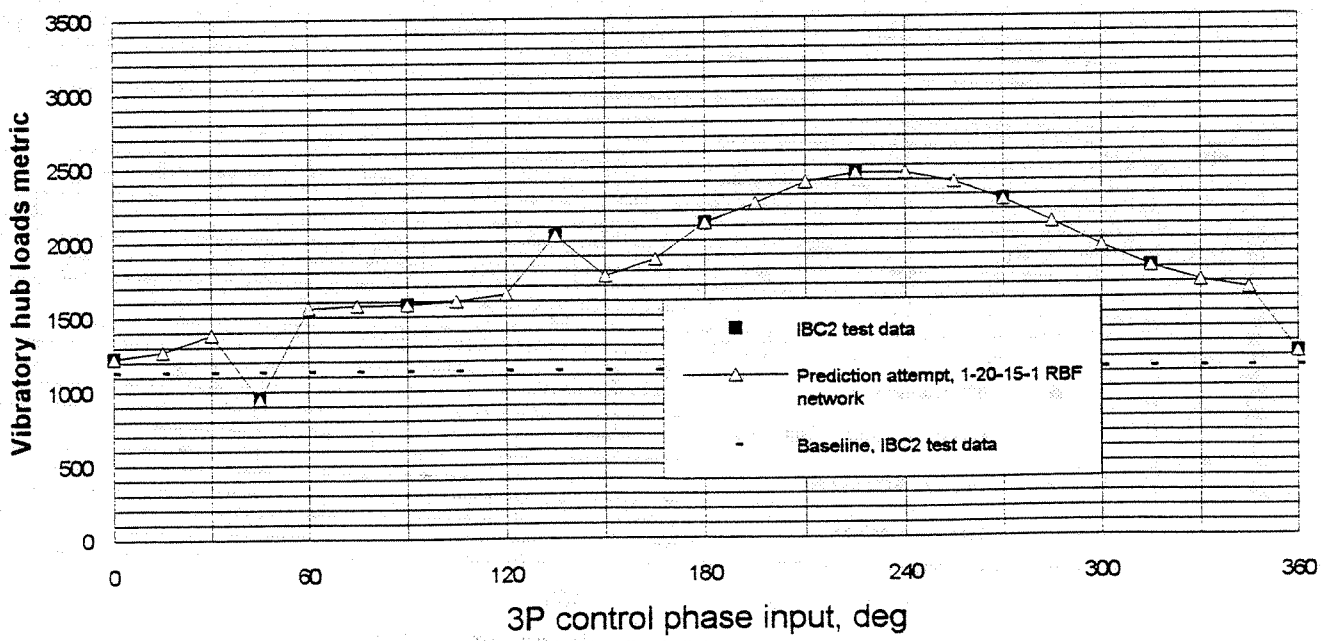

Fig. 16 Case 4: 1-20-15-1 RBF neural network's attempt at modeling and prediction of vibratory hub loads metric, variation with 3P phase, Φ_3 (A_3=0.5 deg)

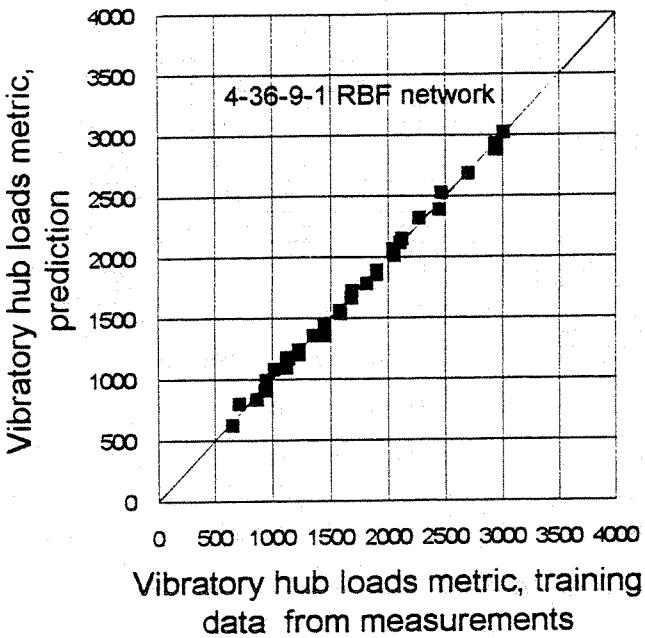

Fig. 17 Four inputs application: Scatter plot of outputs from 4-36-9-1 RBF network versus training data (measured)

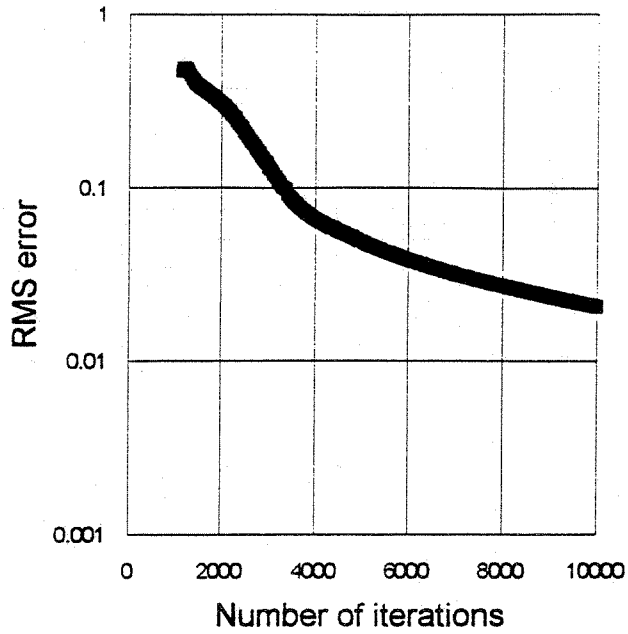

Fig. 18 Four inputs application: RMS error for 4-36-9-1 RBF network

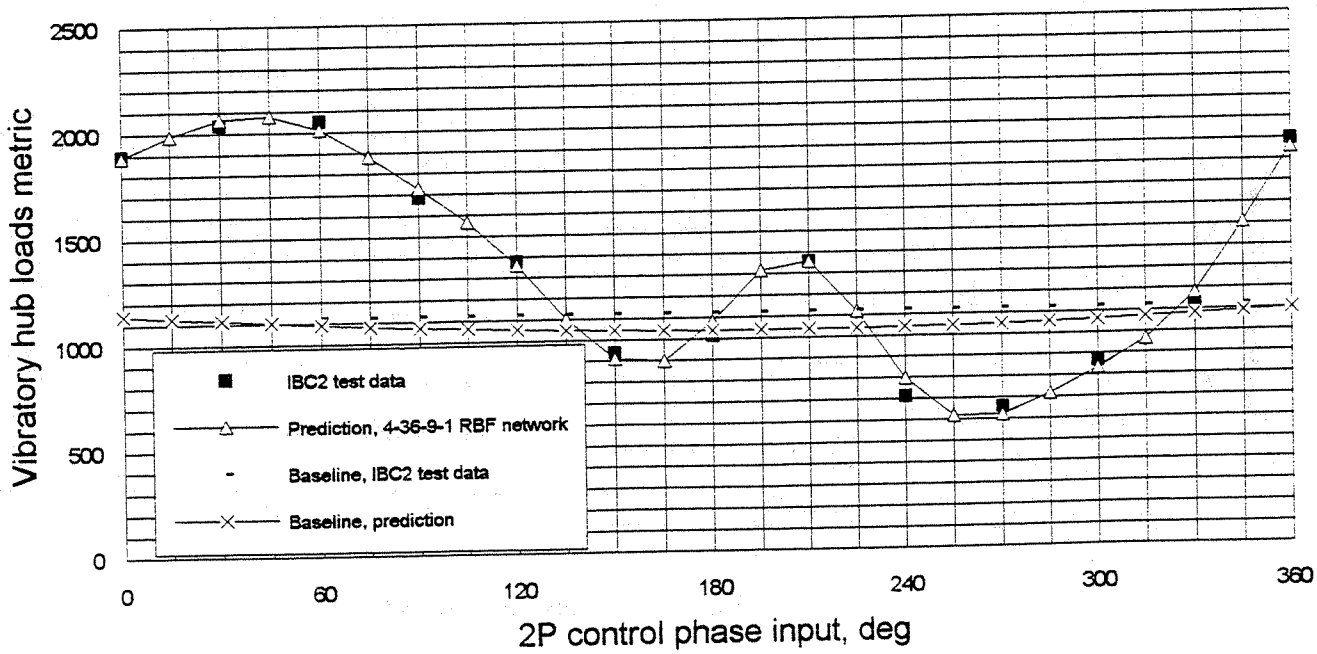

Fig. 19a Four inputs application: 4-36-9-1 RBF neural network modeling and prediction of vibratory hub loads metric, variation with 2P phase, Φ_2 (A_2=1.0 deg, A_3=0 deg); includes baseline prediction

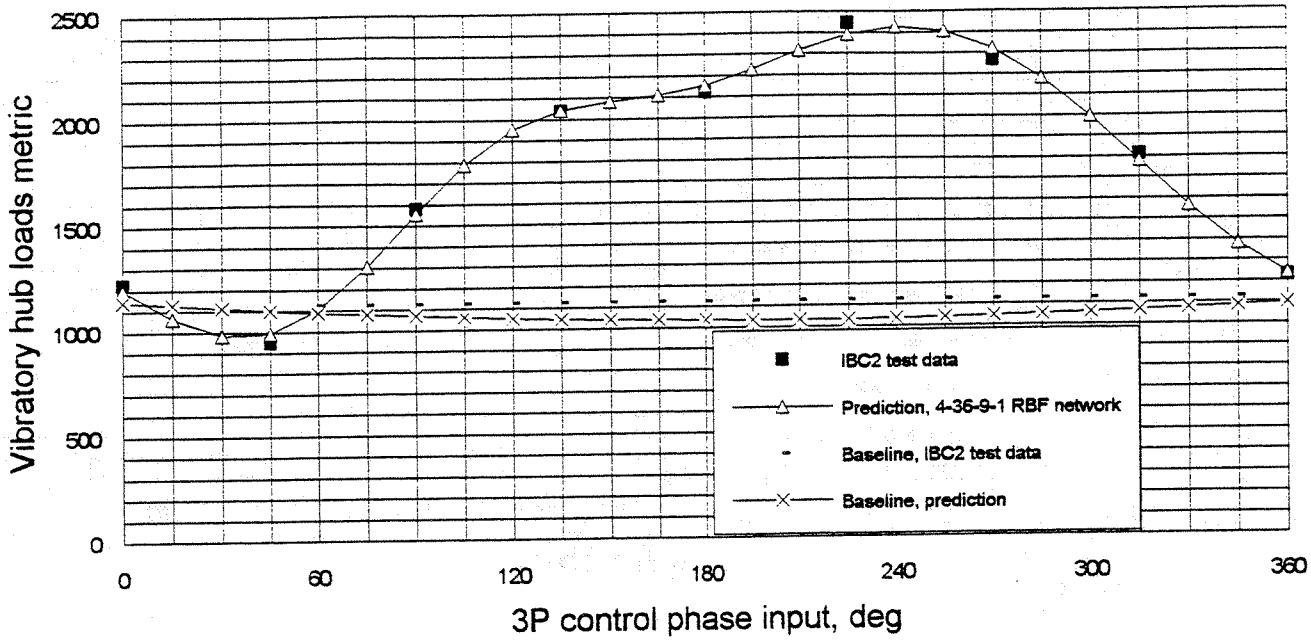

Fig. 19b Four inputs application: 4-36-9-1 RBF neural network modeling and prediction of vibratory hub loads metric, variation with 3P phase, Φ_3 (A_3=0.5 deg, A_2=0 deg); includes baseline prediction

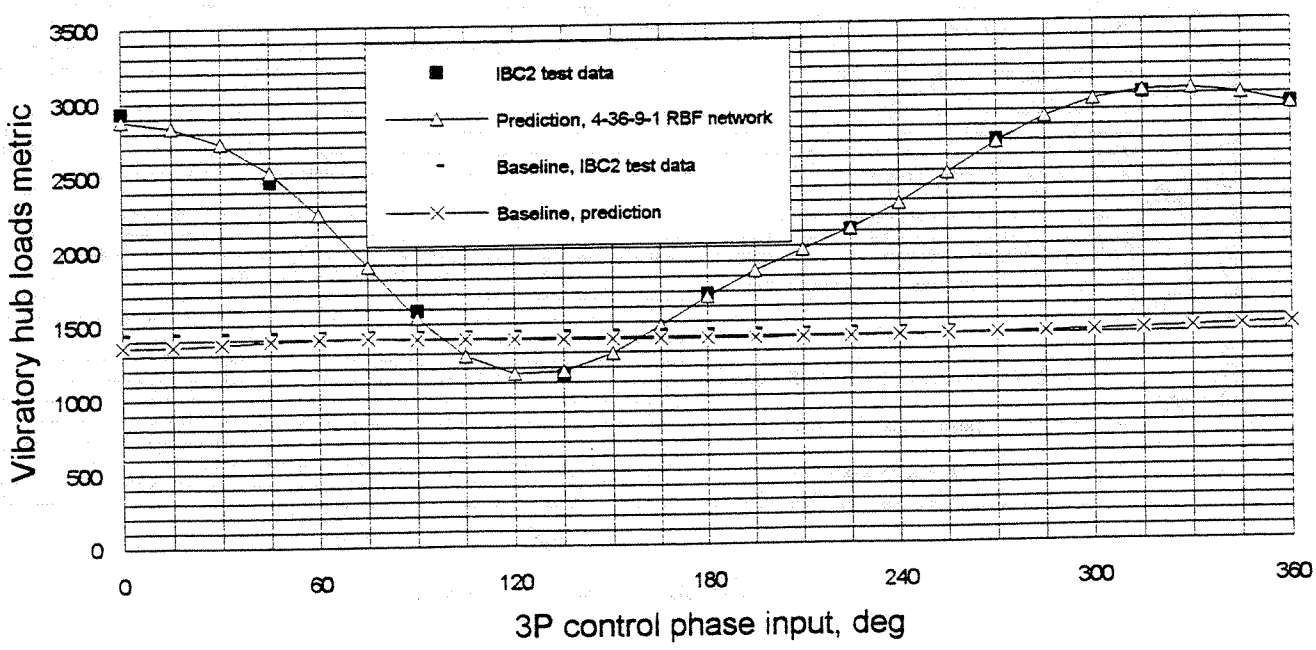

Fig. 19c Four inputs application: 4-36-9-1 RBF neural network modeling and prediction of vibratory hub loads metric, variation with 3P phase, Φ_3 (A_3=0.5 deg, Φ_2=210 deg and A_2=1.0 deg); includes baseline prediction

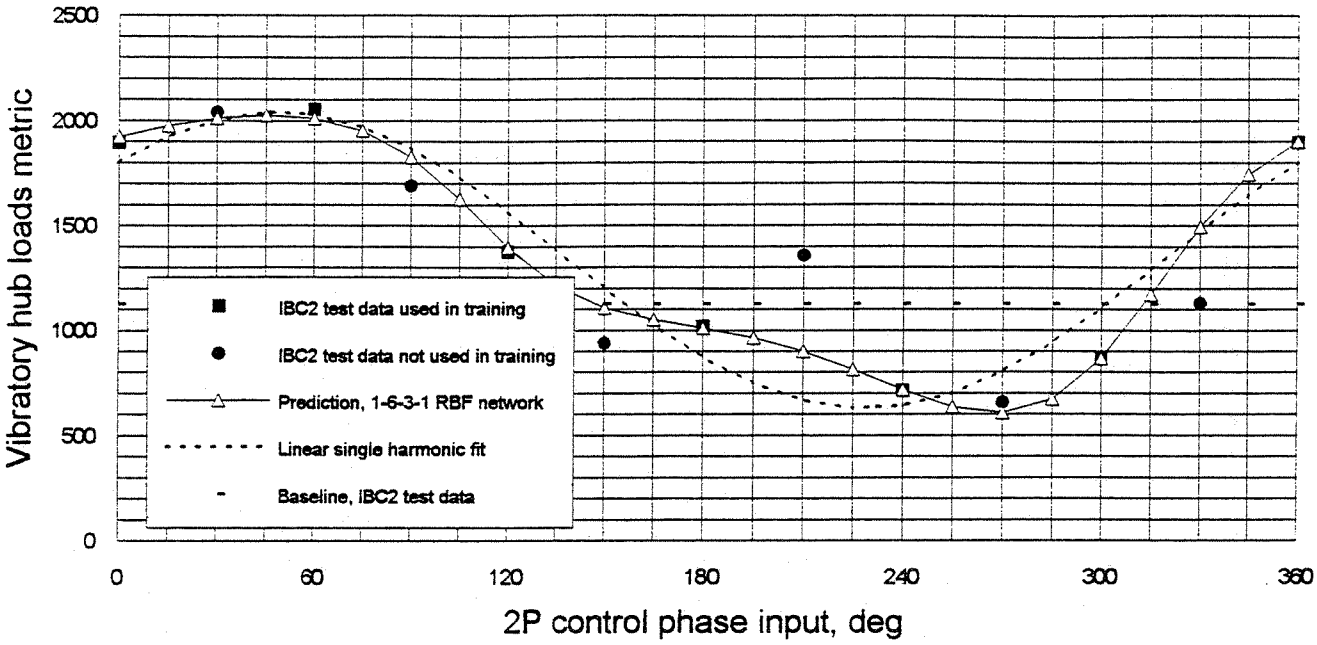

Fig. 20 1-6-3-1 RBF neural network modeling and prediction; 7-pair modeling of Case 1 using data at Φ_2=0, 60, 120, 180, 240, 300, and 360 deg

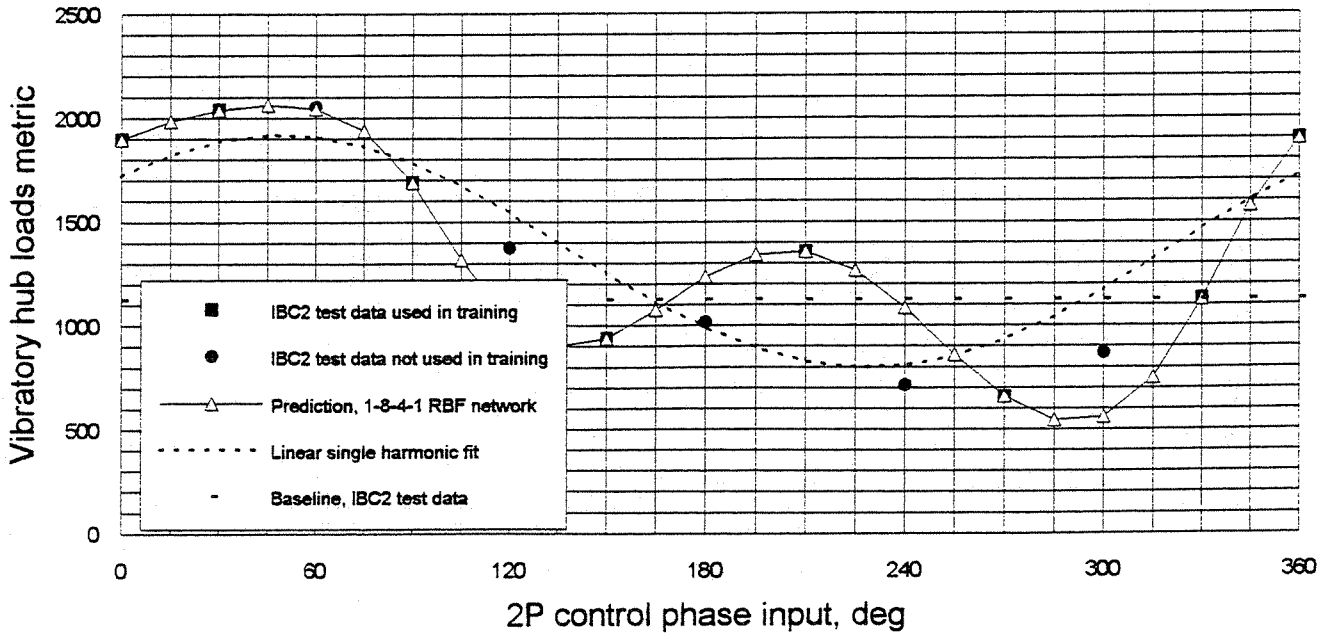

Fig. 21 1-8-4-1 RBF neural network modeling and prediction; 8-pair modeling of Case 1 using data at Φ_2=0, 30, 90, 150, 210, 270, 330, and 360 deg

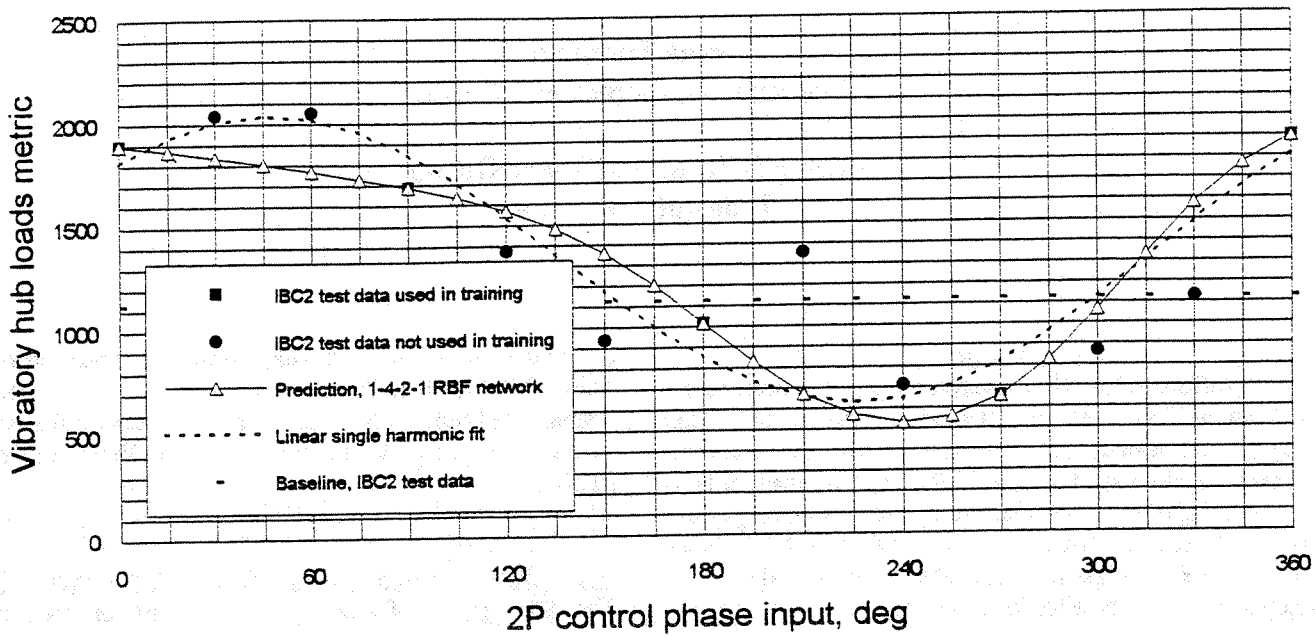

Fig. 22 1-4-2-1 RBF neural network modeling and prediction; 5-pair modeling of Case 1 using data at Φ_2=0, 90, 180, 270, and 360 deg

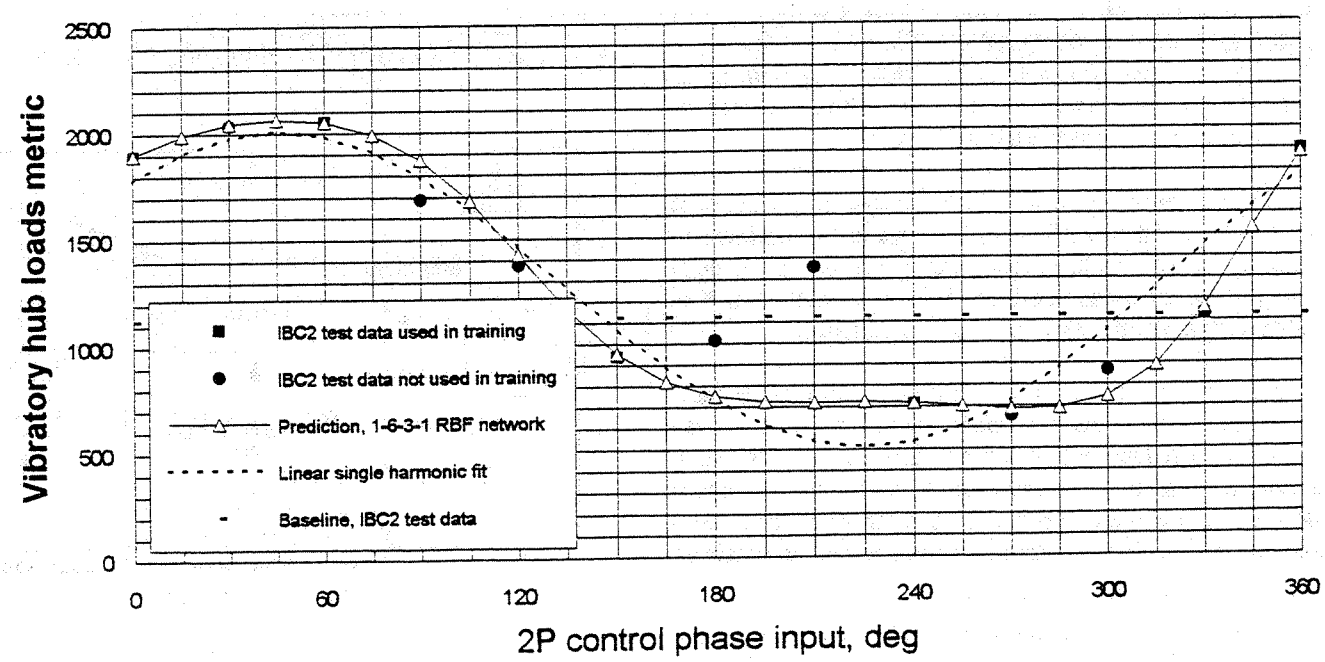

Fig. 23 1-6-3-1 RBF neural network modeling and prediction; 6-pair modeling of Case 1 using data at Φ_2=0, 60, 150, 240, 330, and 360 deg